A thermodynamic tool for designing efficient syntheses of monodisperse and size-tuned nanocrystals

Emanuele Alberto Slejko *, Vanni Lughi

DIA – Department of Engineering and Architecture, University of Trieste, Via Alfonso Valerio 6/1, 34127 Trieste, Italy

ARTICLE INFO

Keywords:
Quantum dots
Colloidal synthesis
Nucleation
Growth
Maximum yield

ABSTRACT

A thermodynamic model based on a modified Classical Nucleation Theory is applied to the formation of colloidal metal and semiconductor nanocrystals. The predictions of the model are compared to experimental results published in the literature and well-established kinetic models, indicating an overall good accuracy. The definition of a potential energy curve that characterizes the system allows the prediction of the final (equilibrium) size of crystals as well as their size distribution. Furthermore, the nucleation process is studied in terms of key parameters affecting the concentration of crystals and is found to be related to the change in critical energy of stable nuclei during nucleation. Threshold values for the nuclei concentrations are predicted, defining instability and metastability conditions for the nucleation process. This model can help in refining our understanding of the mechanisms behind nucleation and growth of nanocrystals, with the goal of optimizing the fabrication process for industrial-scale production of nanocrystals and nanocrystal-based devices.

1. Introduction

Nanocrystals (NCs) are a special class of materials that are particularly important for their functional properties and their potential to revolutionize a multitude of technological areas.[1–3] Their unique properties confer enhanced functions to these materials, playing a fundamental role in novel applications such as analytical sensors, fuel cells, solar cells, biomedical imaging, among many others.[4–6] Their peculiar characteristics mainly arise from the quantum confinement effect, the high exciton coefficients, tunable band gaps and widely controllable emission wavelengths.[3,7,8] Thanks to their increasing adoption, a substantial effort has been produced to optimize and scale-up colloidal synthesis (the main chemical route to produce these materials):[9] batch systems have been researched to process large volumes of NCs, autonomous and continuous reactors have been established and their operations well-documented.[10–14] Novel synthetic routes allow the production of NCs with high quantum efficiency and quantum yield, tailoring their size and narrowing their distribution.[7] One common way to achieve a precise size is to empirically stop the reaction at the right moment;[15] while effective in terms of size control, this results in a low conversion yield synthesis with, often, a sizeable amount of unreacted precursors. The limitations of this approach become important once the cost of the synthesis is considered, as in the case of the industrial production of nanocrystals.

There are several challenges in the synthesis and upscaling of the production process of NCs that have not been addressed yet: for example, the discovery of novel materials and the optimization of the synthetic procedures relies on best practices which are not always backed by a solid experimental and theoretical evidence.[16,17] So far, developments in the optimization of the synthetic procedure have been mainly obtained by empirically changing the synthesis conditions. A better understanding of the chemical and physical processes occurring at the nanoscale would support the definition of effective protocols and general rules.[18] For example, while in general NCs can be fabricated by arrested precipitation methods, obtaining Quantum Dots (QDs) with fairly well controlled size, size dispersion, and tunable bandgaps,[19,20] precise size control, even though fundamental, is often challenging as size variations between batches and low conversion yield are common even with identical starting conditions.[21,22] Such irreproducibility limits the development of novel applications where well-controlled NCs, in terms of size and size distribution, are necessary.[23]

An alternative to the timely arrest of the synthesis consists in letting the reaction reach completion, i.e. maximum yield, and in applying strategies that enable size control of the NCs at the point of full conversion.[24] Some notable contributions have focused attention on the conversion yield of QDs syntheses, developing kinetic models which

* Corresponding author.
E-mail address: easlejko@units.it (E.A. Slejko).

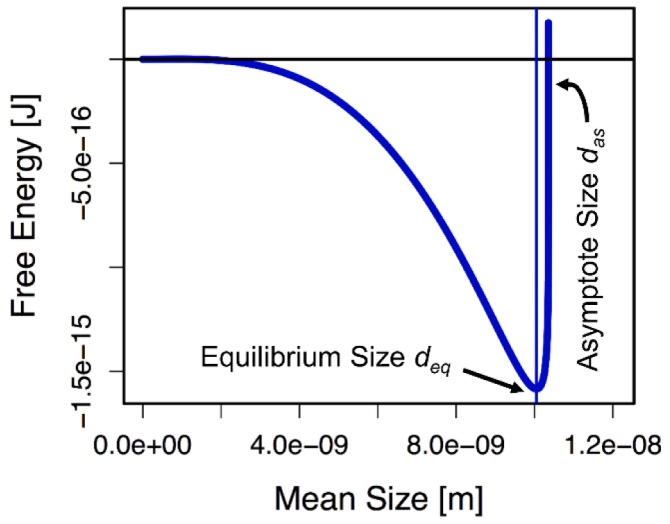

Fig. 1. Example of the modified free energy curve based on Equation (1), calculated for the dataset of Bastùs 2011 [Ref. 54]. The equilibrium size of crystals and the symptote size are indicated.

allow the precise estimation of the final size and distribution.[15,24,25] Unfortunately, these approaches often recur to detailed modelling and precise input data for the evaluation of the nucleation and growth of NCs, parameters that are specific to synthesis conditions and thus cannot be applied to different processes with ease.

One of the most common techniques to obtain uniform NCs with sharp size distribution is recurring to the hot injection synthesis. In this method, a rapid injection of the precursor at high temperature allows the burst nucleation of NCs due to the high value of monomer supersaturation in solution. The size dispersion is limited as long as the nucleation event is kept short. As the supersaturation drops, further nucleation is less probable (as the nucleation rate approaches zero) and only continuous growth of formed crystals can occur, maintaining a sharp size distribution.[15,26–29] The synthesis of uniform nanocrystals is a critical aspect in the production of NCs, as the uniformity of their size, shape and composition guarantees homogeneous properties in the final material; even under the most controlled synthesis conditions, aggregation and ripening have been observed to modify the size distribution right after the nucleation burst.[30–33] Applications that benefit from monodisperse nanocrystals include emitting devices with precise emission wavelengths or self-assembled nanostructures, among many others.[34–38] Growth occurs under several mechanisms, which include monomer attachment, crystals aggregation, coalescence, and oriented attachments among others.[16,32,39–44] The growth pathways are, therefore, not well-understood and well-exploited yet: besides simple monomer attachment, reaction driven growth presents other non-classical mechanisms,[40,45–48] which sensibly influence the final size, composition and shape of NCs.[39] These have the effect of complicating the quantitative predictions of the number, size and the polydispersity in the crystal distribution. The complexity of these mechanisms, along with the need for easily applicable predictive tools for the synthesis performance, suggests further investigation of the process thermodynamics for the comprehension and effective exploitation of the colloidal synthesis of NCs.

2. Experimental Section/Methods

We have performed the analysis recurring to our previously introduced thermodynamic model, based on a modified version of the Classical Nucleation Theory (CNT).[49] The classical formulation of CNT in the case of homogeneous nucleation of quasi-spherical crystals, under the assumption of constant temperature and pressure condition, does not take in consideration the change of supersaturation during the formation of the new phase. To compensate for this, we have introduced a novel term in the Gibbs free energy equation, namely $S(r)$, which represents the amount of monomer available in solution as a function of the crystals growth, and treated it as a substitute for S_0. Basically, the term $S(r)$ is obtained by subtracting from the initial monomer supersaturation S_0 the amount of monomer contained in the solid phase (see Supporting Information). The modified model considers that the supersaturation value, $S(r)$, changes upon the formation of the new solid phase (where r indicates the mean radius of solid crystals), giving rise to a minimum in the free energy curve; the size at which the minimum of the potential energy is located represents the equilibrium size of the crystals. It has been demonstrated that this equilibrium size corresponds to the experimental maximum size of stable particles before the occurrence of aging processes like Ostwald ripening, for example in CdSe NCs.[49]

The equilibrium size represents the minimum in the free energy curve defined by Equation (1) and represented in Fig. 1

$$E(r) = 4\pi r^2\gamma - \frac{4\pi r^3}{3}\frac{RT}{\upsilon} ln\left(S_0 - \frac{4\pi r^3}{3}\frac{N_A C_{NC}}{\upsilon C_s}\right) \quad (1)$$

$E(r)$ indicates the energy required to create a crystal of radius r, γ is the interfacial energy between crystal and solution, R and T are the gas constant and the temperature of the synthesis, respectively. S_0 represents the initial supersaturation, υ is the molar volume of the new phase, C_s is the solubility limit of monomer in solution, N_A indicates the Avogadro's constant, and $C_{NC}(r)$ is the particle concentration of the new phase (number of crystals, expressed as moles per unit volume of the solution). The value C_{NC} is approximated, in our analysis, to a constant representing the total concentration of crystals in suspension, irrespective of size, after nucleation. In this contribution, the equilibrium size of a crystal, d_{eq}, is determined as twice the radius at the minimum of the free energy curve, r_{eq}, derived from Equation (1). At the very first moments after injection, the supersaturation $S(r)$ is essentially equal to the initial value S_0, since the amount of monomers consumed to precipitate the first solid phase is negligible with respect to the overall initial amount, and thus the model is reduced to Classical Nucleation Theory. In a closed system, further precipitation of solid phase by nucleation and/or growth leads to a sensible consumption of the monomer, and the term $S(r)$ decreases significantly. This results in an increase of the free energy of the system -as the impact of the volume term within the free energy equation is mitigated- up to the point where, in proximity of the (unreachable) full conversion of monomers, the free energy curve is limited by a vertical asymptote. The model indicates that sizes larger than the equilibrium diameter are not stable and thus should dissolve, a behavior that, for example, has been observed for certain CdSe syntheses.[50,51] One of the main limitations of the proposed model resides in its spherical approximation for the evaluation of the volume occupied by NCs. Recurring to this approximation makes the model eligible only in evaluating crystals with uniform directional growth.

In this contribution, we intend to expand the applicability of our thermodynamic model, initially developed for CdSe NCs, showing its predictive power in the evaluation of the equilibrium size for CdSe, CdS, PbSe, PbS, Au and Ag NCs. We based our analysis on literature data reporting various techniques for the synthesis of these nanocrystals; this is an important characteristic of our study, as our approach aims to be as general as possible. Only few publications report crystal concentration and size close to the maximum yield point: the majority of scientific contributions about size control recurs to arrested synthesis once the crystals reach the desired size. As the aim of this study is to compare experiments and theoretical calculations, we used data from experimental syntheses in which quasi-spherical nanocrystals have been grown up to the point of maximum monomers conversion.[18,24,25,52–58]

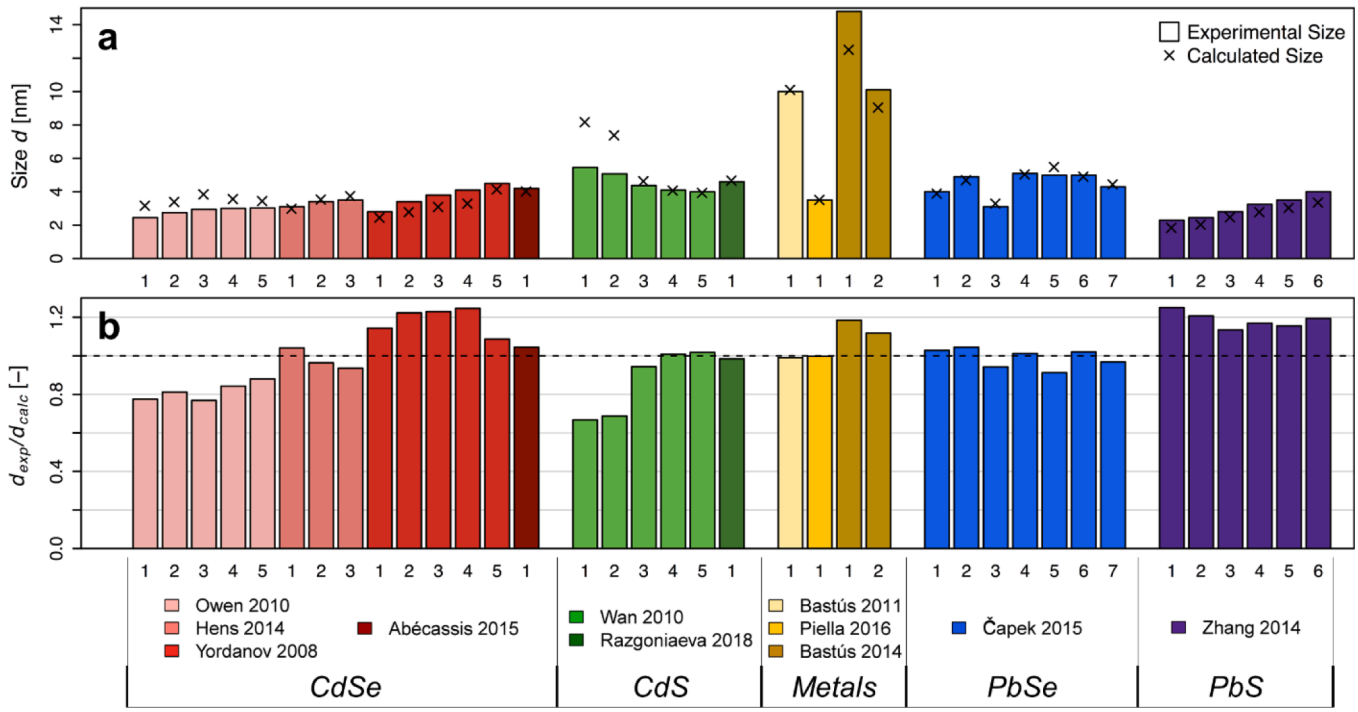

Fig. 2. a) Difference between the experimental size from literature data and predicted size calculated by the thermodynamic model presented here for CdSe, CdS, Au, Ag, PbSe and PbS nanocrystals [Ref. 18,24,25,52–58]. Bars indicate experimental measurements while crosses indicate predictions. b) Ratio between experimental and calculated sizes. The dashed line indicates equal values between experiments and predictions. Input parameters for the calculations are reported in Table S1.

3. Results and discussion

3.1. Equilibrium size

Results of the simulations for the synthesis of CdSe, CdS, PbSe, PbS, Au and Ag are reported in Fig. 2. As can be immediately seen from Fig. 2a, semiconductor quantum dots present experimental sizes in the range of 2–6 nm, while metal nanocrystals can reach up to 14 nm. These differences are related to the exciton Bohr radius of the material, i.e. the crystal size at which quantum confinement becomes evident. The reported sizes are dependent not only on the nature of the material, but also on the synthetic procedure during their fabrication; this is the reason behind the large variation of the reported sizes for CdSe quantum dots, for example. In Fig. 2b bar heights represent the ratio between the experimental and the predicted final (equilibrium) size reported in Fig. 2a. The overall accuracy is very promising: on average, errors are within a factor of less than ± 25%; except for two CdS syntheses. We believe that these experiments may have not reached growth completion, as other syntheses in the CdS dataset by Wan are actually very coherent with our calculations. Equation (1) has been applied to crystals synthesized in the size range from 2 nm to 15 nm, indicating a wide effectiveness of the model in evaluating the size of semiconductor and metal nanocrystals. This size range is technologically very important because, for example, the photoelectronic properties of semiconductor NCs can be modified thanks to the quantum confinement effect. Noble metal nanocrystals with diameters less than 2 nm are gaining increasing attention as well, since their unique physicochemical properties guarantee strong luminescence and superior biocompatibility.[59] Being able to predict the outcome of a synthesis, thus, has direct implications on the final properties of NCs.

Beside their dissimilar compositions and final sizes, all these systems have been experimentally synthesized recurring to distinct techniques and different synthetic conditions (e.g. mechanism of reaction, types and amounts of chemicals, affinity between precursors, and process temperatures among others). The fact that the accuracy is high for all experimental data in Fig. 2 supports the general validity of the proposed approach.

Furthermore, the equilibrium size derived from the model is also consistent with widely accepted and well-established kinetic models, developed for the precursor conversion and growth of nanocrystals in suspension.[16,24,60–62] These kinetic models suggest the existence of a final size once growth had reached completion and before Ostwald ripening or other aggregative aging processes. At that point, these models indicate that the reaction has reached almost full yield and the dispersion is at its lowest level, thus representing the ideal time to stop the reaction.[24] It is worth noting that our results are in accordance with these features. One of the main limitations of well-established kinetic models is that they evaluate the evolution of crystals throughout the entire synthesis, i.e. they quantify nucleation and growth rates concurrently and continuously. Therefore, they rely on a precise physical and chemical characterization of the system and they usually are very intensive in terms of computational power and extremely time-consuming. Our model, on the other side, focuses entirely on the equilibrium condition in a colloidal synthesis: this is an important characteristic, as the equilibrium is mainly influenced by few specific parameters, avoiding the need of complex data as input parameters.[63–65] Furthermore, it is possible to calculate the equilibrium condition with ease as it represents a single critical point in the solution space, cutting down computational time.

The existence of a minimum in the free energy of the system is not an exclusive trait of the colloidal synthesis of nanocrystals; rather, it seems to be a common feature at the nanoscale: water nanobubbles, for instance, have been studied in terms of free energy as a function of their radius of curvature, showing a global minimum which denotes the stable equilibrium state.[66,67] This finding is consistent with our results and indicates the generality of the concept of an equilibrium size in closed systems. At the moment, no data about the concentration of bubbles is available in these studies, meaning that the validity of our model cannot be directly verified, but the similarity of the potential energy curve supports the idea that our model could be extended also to other nucleation events in the physical chemistry world.

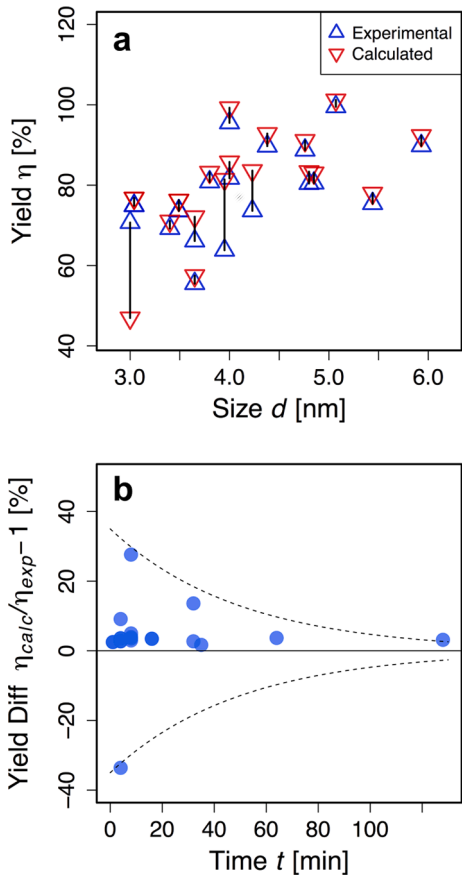

Fig. 3. a) Difference in the experimental [Ref. 25] and predicted yield (Equation (2)) as a function of nanocrystal size. b) Yield differences from panel a) as a function of synthesis time, as indicated in Ref. [25]. Dashed lines are a guide for the eyes. Source data is reported in Table S2.

3.2. Conversion yield

As the most common synthetic approaches are based on the empirical control of the synthesis and the timely arrest of the crystal growth, the conditions are far from optimal in terms of conversion efficiency. [68,69] Synthesizing nanocrystals close to the maximum yield point would be beneficial for the efficient use of materials in the upscaling of synthetic procedures and the industrial adoption of monodispersed nanocrystal production methods.

As the conversion yield represents an important factor in the design of effective synthesis, it is fundamental for our model to provide some functional parameter for estimating it. The conversion yield represents the amount of NCs formed from the starting precursors. It can be expressed as the ratio between the formed NCs size and the maximum size the same number of crystals would have in case of complete conversion of precursors (see Supporting Information). Recurring to the parameters of our model, this last quantity is represented by the crystal size at the vertical asymptote in the free energy curve, i.e. the point where there is no more precursor in solution. Therefore, we can write:

$$\eta_{calc} = \left(\frac{d_{exp}}{d_{as}}\right)^3 \tag{2}$$

where d_{exp} indicates the experimental size reported in Ref. 25, d_{as} is the size corresponding to the vertical asymptote of the Gibbs free energy curve of our model. In their detailed investigation, Čapek and coworkers measured the conversion yield of the synthesis of PbSe via 31P NMR and UV/Vis spectroscopy.[25] Their values have been compared to the predicted yield measured by our model, which has been calculated by Equation (2). Values of the yield derived from our model are very consistent with experimental measurements, except for a few points, as shown in Fig. 3**a**. One possible source of deviation between predicted and experimental yield could be associated with changes in crystal concentration, which may occur during the first stages of NCs growth. It has been observed how the crystal concentration usually increases during nucleation, quickly reaches a maximum and, then, it stabilizes to its final value.[70,71] Often, before stabilizing, a moderate reduction of the crystal concentration is reported; this can be responsible for the deviation of our predicted results from experimental data. In their work, Čapek *et al.* reported that no sensible reduction in the number of nuclei occurred throughout their syntheses, thus the values of crystal concentration provided in their contribution are quite reliable as input for our model and the variation of the crystal concentration cannot be accounted for the deviations. It is worth noting that the highest degree of error is observed for relatively low experimental yield (<80%) and small sizes. This usually happens in syntheses where the kinetics of conversion are still rather fast. As a consequence, the evaluation of input conditions for our model becomes more challenging. In fact, in Fig. 3b we can appreciate how a broader distribution of errors in estimating the conversion yield is found for experimental data associated with the shortest synthesis times. The time reported in Fig. 3b is the one specified in the work by Čapek *et al.* for their experimental growth of NCs.

3.3. Size distribution

Another interesting piece of information provided by the free energy curves is the nanoparticle size dispersion, another key quality indicator of NCs syntheses. We used three sets of size dispersion data obtained from the literature [Ref. 24, 25, 53] and reported in Fig. 4**a**, where both the experimental size dispersion (σ_{exp}) and a parameter σ_{calc}, defined by Equation (4) and linearly dependent on the inverse of the curvature of the free energy curve in proximity of the equilibrium size, k_{eq} (see Fig. S1), are reported for each set of data. The quantities a_0 and a_1 in Equation (4) represent fitting parameters for the calculation of the size dispersion.

$$k_{eq} = \left|\frac{\partial^2 E}{\partial r^2}\right|_{r_{eq}} \tag{3}$$

$$\sigma_{calc} = a_0 + \frac{a_1}{k_{eq}} \tag{4}$$

As further demonstrated in Fig. 4b, the data shows a strong correlation between σ_{exp} and σ_{calc}, suggesting how the free energy curve can become a predictive tool for NCs size dispersion: deeper (and thereby steeper) wells of the free energy curve will be associated with sharper (focused) size distributions, and vice versa - as schematically represented in Fig. 4c.

3.4. Nucleation stage

The size distribution can be related, beside to the equilibrium size, to the critical size as well: in fact, the distribution of the second derivative of the potential curve calculated in the critical size, k_{cr}, is almost the same as the distribution of the second derivative in the equilibrium point, k_{eq}, Fig. S2. This is reasonable, since it is during nucleation that stable nuclei are formed with their characteristic distribution. Furthermore, the fact that both k_{eq} and k_{cr} can be seen as good predictors of the final size distribution suggests that, under a thermodynamic perspective, the size distribution cannot be modified sensibly during growth, at least not without a simultaneous modification in the concentration of crystals. As nucleation has a strong influence on the size dispersion of the final crystals, controlling its progress is critical. Experimental evidence has proved that - before the occurrence of aging processes such as the Ostwald ripening - as the number of nanocrystals grows, the majority of

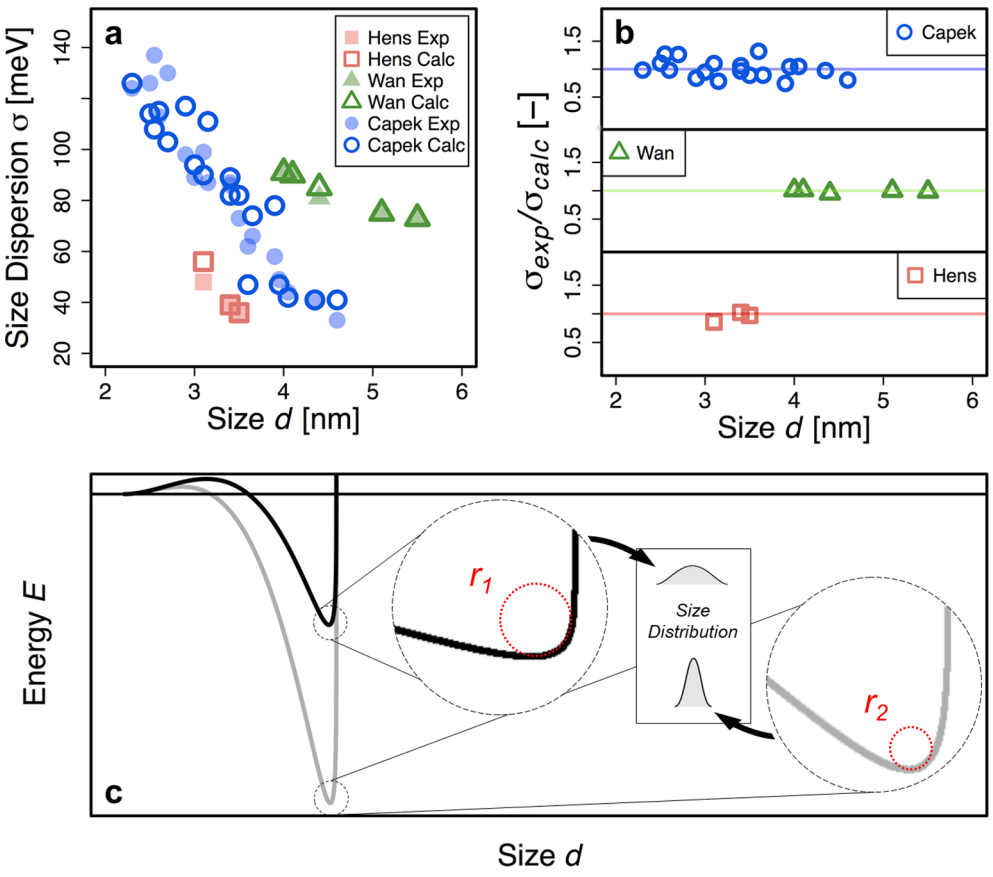

Fig. 4. Correlation between experimental size dispersion and the shape of the free energy curves. a) Experimental and calculated (by means of Equation (4)) size dispersion, as a function of NCs size, for each of the three datasets [Ref. 24, 25, 53]. Source data is reported in Table S3. b) Ratio between the experimental dispersion σ_{exp} and the calculated one σ_{calc} as reported in panel a). c) Schematic representation of the relationship between size dispersion and curvature of the free energy curve at the curve minimum.

monomer is consumed for the growth of these crystals rather than for the nucleation of new nuclei.[24] The time required for growth to overtake nucleation can be tuned by controlling the amount of monomer consumed during the first stages of nucleation. In fact, if the monomer consumption rate is large, the threshold for switching from nucleation to growth will be reached early, since the resulting reduction of the nucleation rate, G_n, would be faster. The event of growth overtaking nucleation can be related to the increase of the energy barrier for nucleation.

In this context, we propose an alternative approach for modelling the nucleation stage, focused on the variation of the potential energy during the formation of crystals. While new phase is formed, since part of the precursors is transferred to stable nuclei, the thermodynamic conditions for sustaining further nucleation get increasingly less favorable.[72] In terms of the potential energy, this behavior is represented by an increase of the critical size and critical energy due to precursor consumption (Fig. 5**a**). Fig. 5b illustrates how the variation of the energy barrier influences the final crystal concentration: since the nucleation rate has a strong exponential dependence on the critical energy, we assume that the nucleation rate rapidly approaches zero when the critical energy approaches a threshold value. It turns out that, modelling the nucleation in terms of $\partial E/\partial C_{NC}$, allows us to easily identify the most important parameters to control the number of nuclei formed and, consequently, the equilibrium size and the size dispersion. This is an important advancement, as usually the nucleation process was addressed in terms of the nucleation rate (G_n=$\partial C_{NC}/\partial t$), with the inconvenience that the final number of crystals formed is not readily accessible. Recurring to the formulation of $\partial E_{cr}/\partial C_{NC}$ from our model (Equation (7)), we can observe that, for example, an increase in C_0 would reduce the value of the derivative, resulting in an increase of the concentration of crystals formed once the threshold value E_{cr} is reached. The opposite reasoning applies to C_s, as an increase of this parameter would reduce the final concentration of nuclei. These two parameters have been experimentally studied by Owen and coworkers and by Abe *et al.*; their findings are coherent with the result of our predictions (trends reported in Fig. 5c-d).[15,52,73]

$$r_{cr} \cong \frac{2\nu\gamma}{RTln(S_0)} \tag{5}$$

$$E_{cr} = 4\pi r_{cr}^2\gamma - \frac{4}{3}\frac{\pi r_{cr}^3 RT}{\nu} ln\left(S_0 - \frac{4}{3}\frac{\pi r_{cr}^3 N_A C_{NC}}{\nu C_s}\right) \tag{6}$$

$$\frac{\partial E_{cr}}{\partial C_{NC}} = \frac{\left(\frac{4\pi r_{cr}^3}{3\nu}\right)^2 RN_A T}{C_0 - C_s - \frac{4\pi r_{cr}^3 N_A C_{NC}}{3\nu}} \tag{7}$$

$$E_{cr0} = 4\pi r_{cr}^2\gamma - \frac{4}{3}\frac{\pi r_{cr}^3 RT}{\nu} ln\left(\frac{C_0}{C_s} - 1\right) \tag{8}$$

Temperature has a dual influence: while on the one hand an increase in temperature is associated with a reduction of the initial critical energy, i.e. the critical energy when no crystals have precipitated yet ($E_{cr}(C_{NC} = 0) = E_{cr0}$, defined by Equation (8)), on the other hand it increases the value of the derivative in Equation (7). A possible representation of the effect of increasing temperature is shown in Fig. 5e, where the presence of a cross-over point is indicated. This point suggests that, even with favorable initial conditions for nucleation (low E_{cr0}), the final concentration of nuclei can be lower. This could be an interpretation for the data of Yordanov,[58] for example, where increments in temperature resulted in fewer nuclei formed. It is worth noting that the trends in Fig. 5e result from simulations where only temperature has been changed; in a real synthesis, it is very unlikely that the other parameters will not be affected by a temperature change. The mutual influence of T, C_0 and C_s is still under investigation.

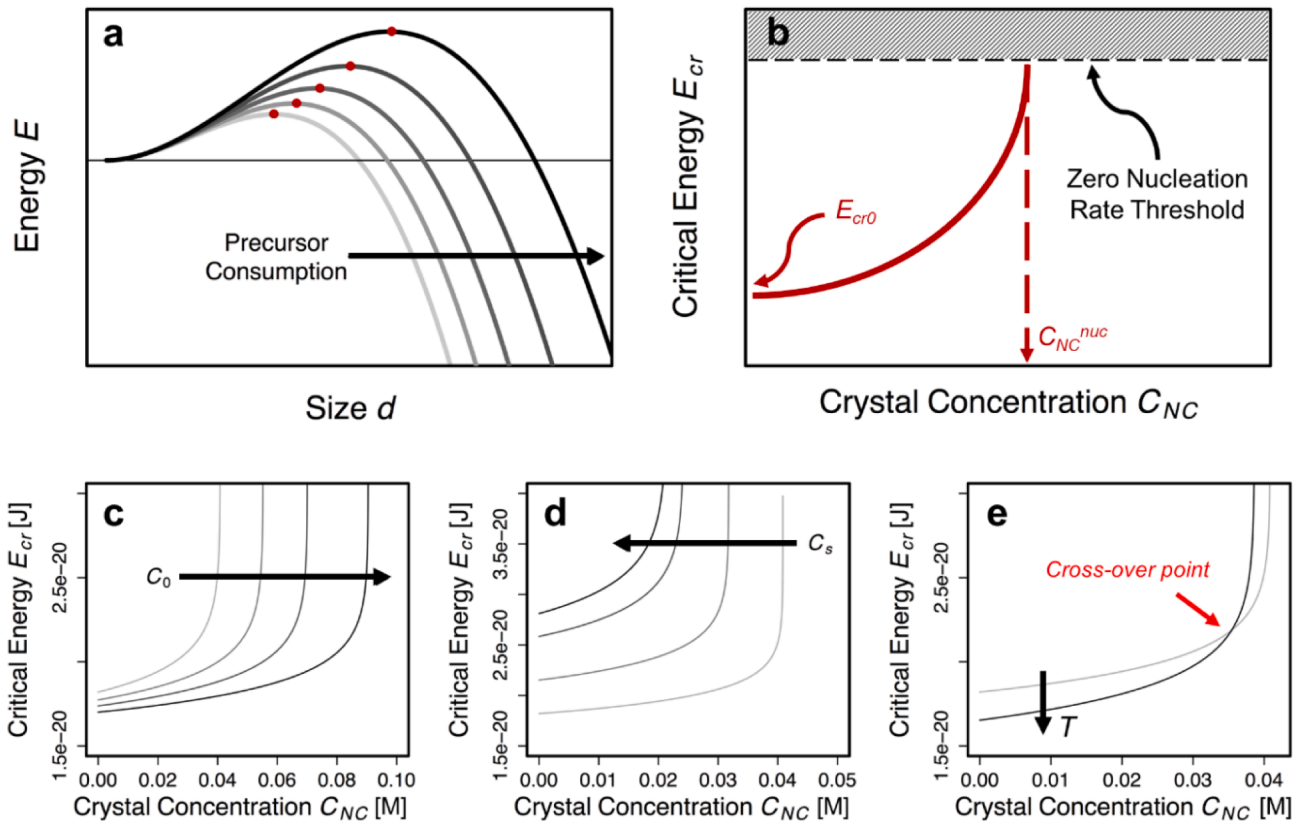

Fig. 5. a) Change of the potential energy curve in proximity of the critical point, as a function of precursor consumption. Because of precursor consumption, as nucleation progresses the local maximum (red dots) shifts towards higher energies and larger sizes. b) Change of the critical energy (Equation (6)) upon formation of new nuclei according to our model (the red curve is essentially a continuous representation of the red dots in panel a). When the value of the critical energy reaches a threshold value, the nucleation rate drops dramatically. c) The calculated critical energy curve (Equation (6)) is shown as a function of the initial monomer concentration. d) Influence of the crystal solubility on the critical energy curve (Equation (6)). e) The critical energy curve (Equation (6)) as a function of temperature. The cross-over point indicates the possibility of obtaining fewer crystals even if nucleation is initially favored (lower E_{cr0}). (For interpretation of the references to colour in this figure legend, the reader is referred to the web version of this article.)

Table 1
Effects of a change in the indicated parameters on the crystal concentration, equilibrium size and size distribution, as predicted by the proposed model. The effect of temperature on the crystal concentration is dual, in accordance to the discussion in the main text.

Parameter	Change	Effect on C_{NC}	Effect on d_{eq}	Effect on σ_{sim}
Initial monomer concentration C_0	↑	↑	↓	↑
Interfacial energy of crystals γ	↑	↓	↑	↓
Solubility of monomer C_s	↑	↓	↑	↓
Temperature T	↑	↑↓	↓	↑

Experimental investigations have been carried out on the effects of free ligand concentration, initial precursor concentration, solubility of the solute and conversion of monomers, and diffusion coefficient of the solute.[15,41,33,73,74] Accordingly, our model identifies the majority of these synthetic conditions as variables for tuning the potential energy curve, interpreting their effect under a thermodynamic point of view (Table 1).

Additionally, this potential energy curve interpretation allows us to identify the conditions that promote a sharp size distribution in an intriguing fashion: the number of crystals formed during nucleation influences the curvature of the potential energy curve, and we have previously discussed how the second derivative of the free energy curve is associated to the size dispersion of crystals.

Several reports show that, during growth, the size distribution of nanocrystals usually gets narrower.[75,76] Particle dissolution or coalescence may be responsible of focusing of the size distribution observed during these syntheses:[40,41] as a fraction of crystals disappear, the mean equilibrium size gets larger thanks, for example, to the novel amount of monomer available. At the same time, due to the reduction in C_{NC}, the free energy curve at equilibrium becomes deeper and its second derivative value in d_{eq} becomes larger, thus promoting a narrower size distribution and the observed focusing behavior. Furthermore, this effect is also in accordance with the kinetics regulated by the classical definition of the size dependent growth rate:[60,65,78] the net reduction of the number of nuclei would lower the size at which maximum growth rate is observed, thus promoting the well-known focusing mechanism. It is worth mentioning that, based on our model, no change in the size distribution can take place without a concomitant reduction in crystal concentration. Coalescing of nanoparticles can be more important than monomer attachment in the final stages of nucleation/first stages of growth, and it has been observed that it occurs even on crystals well stabilized by ligands and capping agents.[16,45,60] The coalescence mechanisms of nanocrystals has a strong impact on the number of particles, as reductions up to 30% have been observed. Our model provides an interpretation of experimental data showing the concurrent reduction of the number of crystals and sharpening of size distribution, adding a thermodynamic perspective to these experimental observations.

The increment of the critical energy associated to the formation of stable crystals during nucleation in a closed system is linked to the simultaneous reduction of the mean equilibrium size and increment of the free energy at equilibrium, depicted in Fig. 6**a**. Thus, theoretically,

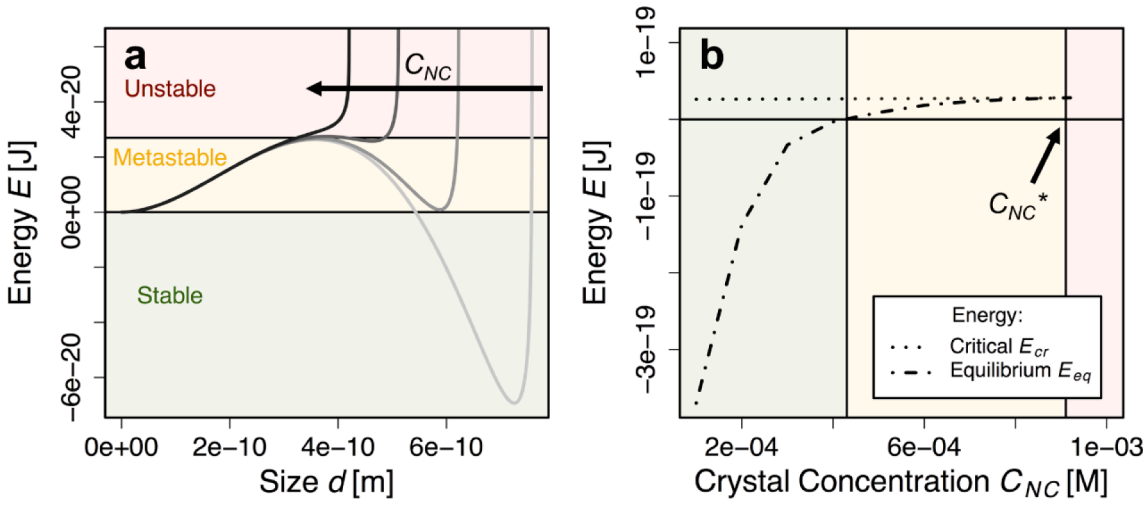

Fig. 6. The effect of crystal concentration on the free energy of the system: a) the potential energy curve reaches the local minimum at a smaller size upon increasing the concentration of crystals. Depending on the values of the free energy at equilibrium, three different regions can be defined. b) Trends of the critical and equilibrium energy as a function of the crystal concentration. The point where the two energies are equal is the threshold crystal concentration C_{NC}*.

each nucleation phase presents a threshold value of the crystal concentration, C_{NC}*, corresponding to the point where the free energy associated to the equilibrium size matches the one at critical size, i.e. $E_{eq}(C_{NC}^*) = E_{cr}(C_{NC}^*)$ (see Fig. 6b). Nucleation for concentration of crystals larger than the threshold value is not possible, as the nuclei would be unstable. Furthermore, before reaching the threshold value, a metastable region is present for $0 < E_{eq}(C_{NC}) < E_{cr}(C_{NC})$: for nuclei concentrations included within this range, the nucleation of particles with a size larger than the critical one is possible, but size fluctuations can lead to re-dissolution of the solid phase, as the minimum of the free energy curve is larger than the energy of the system in the liquid phase. Approximated analytical forms for the critical and metastable concentrations of crystals are provided in the Supporting Information.

The threshold crystal concentration is an important parameter even outside the nucleation stage: when the system is not stable for a certain crystal concentration, which is larger than the threshold value, we expect balancing mechanisms like coalescence of crystals to occur. This is what usually happens, for example, on colloidal nanocrystals that are not stable enough in the specific ligand-solvent combination: the instability is balanced by response mechanisms like aggregation of crystals, lowering the potential of the system and possibly causing precipitation of the solute. The definition of this threshold concentration is technologically very important, as it allows us to have a finer control on the stability of crystals in suspension. Furthermore, Razgoniaeva et al. observed the existence of a thermal threshold for coalescence while synthesizing CdS, CdSe, $CsPbBr_3$ and $CuZnSnS_4$ nanocrystals.[41] They reported significant changes in average particle diameter at reaction temperature above a certain threshold value, with the concurrent addition of new ligands to the solution. Their results can be interpreted by the concept of C_{NC}*, as illustrated in Fig. S3.

3.5. *Maps for optimal synthesis conditions*

For the synthesis of nanocrystals, the maximum reaction yield is the measured amount of solid product in equilibrium with the solution. At the nanoscale, crystal size effects come to play which modify the free

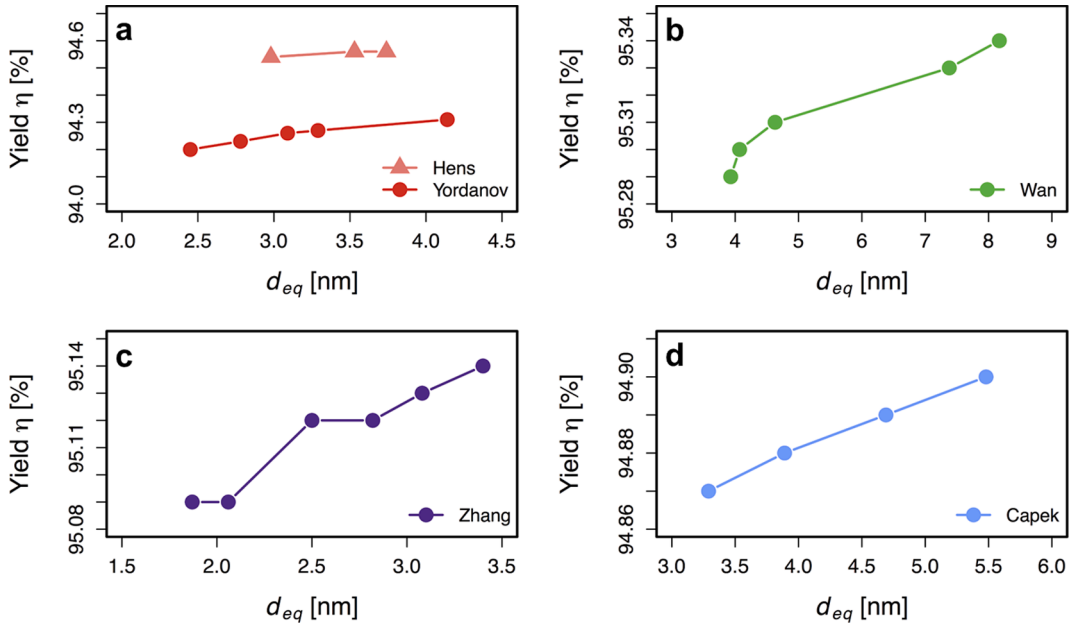

Fig. 7. Trends of conversion yield with equilibrium size for different systems: a) CdSe, b) CdS, c) PbS, d) PbS.

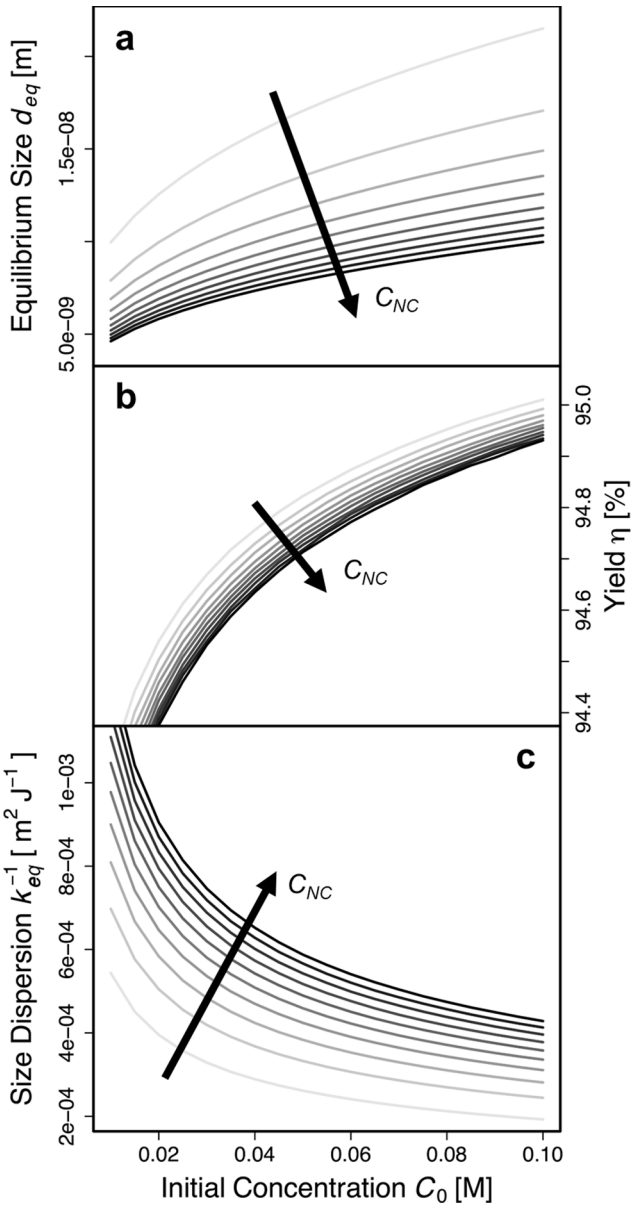

Fig. 8. Equilibrium maps. Curves indicate a) equilibrium size, b) yield and c) size dispersion as a function of initial monomer concentration and crystal concentration.

energy of the system and, as a result, the equilibrium is altered compared to the macroscopic scale. The increase of free energy of the solid phase due to crystal specific surface area (i.e., the ratio of the surface area on the volume of a crystal) pushes the equilibrium point towards smaller sizes and, thus, lower yields. This effect is related to the Ostwald-Freundlich equation, i.e. the solubility of crystals increases as the crystal size decreases.[78]

The influence of the calculated equilibrium size on yield, derived from the application of experimental data to the proposed thermodynamic model, is shown in Fig. 7**a-d**. For all systems, the smaller the specific surface area of the crystal, the higher the maximum yield, in accordance to the reasoning described above.

In addition, this data shows consistent differences in the synthetic techniques: for example, considering data by Hens and coworkers and comparing it to the work of Yordanov *et al.*, thermodynamic calculations forecast a higher yield for the synthesis of Hens, even if size and crystal concentration are quite similar in both datasets (Fig. S4). In this specific case, we speculate that it could be the result of a higher initial monomer concentration and, consequently, faster reaction rates. In fact, Abe and Čapek estimated that the reaction rate is proportional to the monomer concentration.[15]

With all of these findings, we can define thermodynamic charts which support us in the synthesis of monodisperse and size-tuned NCs. A straightforward observation from Fig. 8 is that a higher initial monomer concentration favors the efficient synthesis of large and monodisperse crystals. This is a promising indication of the future potential of large-scale industrial productions. In this context, the influence of the nucleation stage is extremely important as a large crystal concentration counterbalances the benefits of the initial monomer concentration, decreasing crystal size and synthesis efficiency and increasing size dispersion. The numerical predictions in Fig. 8 are obtained investigating how individual parameters affect the equilibrium condition but, usually, they mutually interact concurrently (for example, it is unlikely that a higher initial monomer concentration does not promote a higher crystal concentration after nucleation). At this time, it is difficult to discuss combinations of parameters, since their mutual influence is still under investigation. Nonetheless, this analysis can pave the way for a more precise understanding of the techniques for the industrial production of colloidal nanocrystals.

4. Conclusion

In this contribution, we have extended the validity of the modified version of Classical Nucleation Theory, expressed by Equation (1), for the evaluation of the equilibrium size of metal and semiconductor nanocrystals synthesized by various techniques.[75] The modified thermodynamic theory points to a number of strategies for controlling the size of stable crystals, helping to identify a few key parameters in the synthesis setup, an advantage in terms of accuracy and computational time in contrast with common and well-established kinetic models. The consistency of the results has been demonstrated by comparing them with experimental data in terms of size and conversion yield.

We have observed that the shape of the free energy curve, expressed as the second derivative of the curve and calculated at the equilibrium size, can be associated to the size distribution of the crystals, with larger values of the derivative (more concave curve) associated to sharper size distributions. We have also noticed that the focusing behavior, observed in a multitude of syntheses after the nucleation stage, takes place with a simultaneous reduction of the crystal concentration due to coalescence or aggregation. This reduction of the crystal concentration can be interpreted as the existence of an instability region, where coalescence, for example, is one mechanism for the reduction of the potential energy and the migration towards a more stable configuration. One major limitation in the proposed model resides in the need for the crystal concentration as input parameter. Unfortunately, even well-established kinetic models fail to accurately evaluate the crystal concentration within their calculations, as this remains one of the major challenge in the modelling of the mechanisms of nucleation and growth.

Furthermore, the modified thermodynamic model allows us to compare different techniques and evaluate their impact on NCs size and size distribution. From these considerations, the development of equilibrium maps is viable and it permits to recognize the optimal conditions for the efficient production of monodisperse and size-tunable nanocrystals, a topic of utmost importance for the large-scale fabrication of NCs-based devices.

CRediT authorship contribution statement

Emanuele Alberto Slejko: Conceptualization, Methodology, Validation, Formal analysis, Writing – original draft, Writing – review & editing, Visualization. **Vanni Lughi:** Writing – original draft, Supervision.

Declaration of Competing Interest

The authors declare that they have no known competing financial interests or personal relationships that could have appeared to influence the work reported in this paper.

Data availability

Data will be made available on request.

Appendix A. Supplementary data

Supplementary data to this article can be found online at https://doi.org/10.1016/j.commatsci.2022.111887.

References

[1] D.V. Talapin, J.-S. Lee, M.V. Kovalenko, E.V. Shevchenko, Prospects of Colloidal Nanocrystals for Electronic and Optoelectronic Applications, Chem. Rev. 110 (1) (2010) 389–458.

[2] M.V. Kovalenko, L. Manna, A. Cabot, Z. Hens, D.V. Talapin, C.R. Kagan, V. I. Klimov, A.L. Rogach, P. Reiss, D.J. Milliron, P. Guyot-Sionnnest, G. Konstantatos, W.J. Parak, T. Hyeon, B.A. Korgel, C.B. Murray, W. Heiss, Prospects of Nanoscience with Nanocrystals, ACS Nano 9 (2) (2015) 1012–1057.

[3] C.R. Kagan, E. Lifshitz, E.H. Sargent, D.V. Talapin, Building Devices from Colloidal Quantum Dots, Science 2016, 353 (6302), aac5523-1–aac5523-9.

[4] S. Guo, E. Wang, Noble Metal Nanomaterials: Controllable Synthesis and Application in Fuel Cells and Analytical Sensors, Nano Today 6 (3) (2011) 240–264.

[5] X. Chen, S. Shen, L. Guo, S.S. Mao, Semiconductor-Based Photocatalytic Hydrogen Generation, Chem. Rev. 110 (11) (2010) 6503–6570.

[6] D. Bera, L. Qian, T.-K. Tseng, P.H. Holloway, Quantum Dots and Their Multimodal Applications: A Review, Materials 3 (4) (2010) 2260–2345.

[7] N.K. Ozdemir, J.P. Cline, C.J. Kiely, S. McIntosh, M.A. Snyder, Scalable Biomineralization of CdS Quantum Dots by Immobilized Cystathionine γ-Lyase, ACS Sustain. Chem. Eng. 8 (40) (2020) 15189–15198.

[8] M. Alizadeh-Ghodsi, M. Pourhassan-Moghaddam, A. Zavari-Nematabad, B. Walker, N. Annabi, A. Akbarzadeh, State-of-the-Art and Trends in Synthesis, Properties, and Application of Quantum Dots-Based Nanomaterials, Part. Part. Syst. Charact. 36 (2) (2019), pp. 1800302–1–1800302-20.

[9] S.G. Kwon, T. Hyeon, Formation Mechanisms of Uniform Nanocrystals via Hot-Injection and Heat-Up Methods, Small 7 (19) (2011) 2685–2702.

[10] J.I. Kim, J.-K. Lee, Sub-Kilogram-Scale One-Pot Synthesis of Highly Luminescent and Monodisperse Core/Shell Quantum Dots by the Successive Injection of Precursors, Adv. Funct. Mater. 16 (16) (2006) 2077–2082.

[11] C.-X. Zhao, L. He, S.Z. Qiao, A.P.J. Middelberg, Nanoparticle Synthesis in Microreactors, Chem. Eng. Sci. 66 (7) (2011) 1463–1479.

[12] Y. Song, J. Hormes, C.S.S.R. Kumar, Microfluidic Synthesis of Nanomaterials, Small 4 (6) (2008) 698–711.

[13] E.M. Chan, C. Xu, A.W. Mao, G. Han, J.S. Owen, B.E. Cohen, D.J. Milliron, Reproducible, High-Throughput Synthesis of Colloidal Nanocrystals for Optimization in Multidimensional Parameter Space, Nano Lett. 10 (5) (2010) 1874–1885.

[14] P.L. Saldanha, V. Lesnyak, L. Manna, Large Scale Syntheses of Colloidal Nanomaterials, Nano Today 12 (2017) 46–63.

[15] S. Abe, R.K. Čapek, B. De Geyter, Z. Hens, Reaction Chemistry/Nanocrystal Property Relations in the Hot Injection Synthesis, the Role of the Solute Solubility, ACS Nano 7 (2) (2013) 943–949.

[16] F. Wang, V.N. Richards, S.P. Shields, W.E. Buhro, Kinetics and Mechanisms of Aggregative Nanocrystal Growth, Chem. Mater. 26 (1) (2014) 5–21.

[17] R.E. Schaak, M.E. Williams, Full Disclosure: The Practical Side of Nanoscale Total Synthesis, ACS Nano 6 (10) (2012) 8492–8497.

[18] B. Abécassis, C. Bouet, C. Garnero, D. Constantin, N. Lequeux, S. Ithurria, B. Dubertret, B.R. Pauw, D. Pontoni, Real-Time in Situ Probing of High-Temperature Quantum Dots Solution Synthesis, Nano Lett. 15 (4) (2015) 2620–2626.

[19] N. Reilly, M. Wehrung, R.A. O'Dell, L. Sun, Ultrasmall Colloidal PbS Quantum Dots, Mater. Chem. Phys. 147 (1–2) (2014) 1–4.

[20] T.-Y. Liu, M. Li, J. Ouyang, M.B. Zaman, R. Wang, X. Wu, C.-S. Yeh, Q. Lin, B. Yang, K. Yu, Non-Injection and Low-Temperature Approach to Colloidal Photoluminescent PbS Nanocrystals with Narrow Bandwidth, J. Phys. Chem. C 113 (6) (2009) 2301–2308.

[21] A. Preske, J. Liu, O.V. Prezhdo, T.D. Krauss, Large-Scale Programmable Synthesis of PbS Quantum Dots, ChemPhysChem 17 (5) (2016) 681–686.

[22] C.M. Evans, M.E. Evans, T.D. Krauss, Mysteries of TOPSe Revealed: Insights into Quantum Dot Nucleation, J. Am. Chem. Soc. 132 (32) (2010) 10973–10975.

[23] A. Preske, S.W. O'Neill, B.D. Swartz, J. Liu, O.V. Prezhdo, T.D. Krauss, Size-Programmed Synthesis of PbSe Quantum Dots via Secondary Phosphine Chalcogenides, Chem. Mater. 31 (20) (2019) 8301–8307.

[24] Z. Hens, R.K. Čapek, Size Tuning at Full Yield in the Synthesis of Colloidal Semiconductor Nanocrystals, Reaction Simulations and Experimental Verification, Coord. Chem. Rev. 263–264 (1) (2014) 217–228.

[25] R.K. Čapek, D. Yanover, E. Lifshitz, Size Control by Rate Control in Colloidal PbSe Quantum Dot Synthesis, Nanoscale 7 (12) (2015) 5299–5310.

[26] C.B. Murray, D.J. Norris, M.G. Bawendi, Synthesis and Characterization of Nearly Monodisperse CdE (E = Sulfur, Selenium, Tellurium) Semiconductor Nanocrystallites, J. Am. Chem. Soc. 115 (19) (1993) 8706–8715.

[27] D.V. Talapin, A.L. Rogach, A. Kornowski, M. Haase, H. Weller, Highly Luminescent Monodisperse CdSe and CdSe/ZnS Nanocrystals Synthesized in a Hexadecylamine−Trioctylphosphine Oxide−Trioctylphospine Mixture, Nano Lett. 1 (4) (2001) 207–211.

[28] J. Jasieniak, C. Bullen, J. van Embden, P. Mulvaney, Phosphine-Free Synthesis of CdSe Nanocrystals, J. Phys. Chem. B 109 (44) (2005) 20665–20668.

[29] M.A. Hines, G.D. Scholes, Colloidal PbS Nanocrystals with Size-Tunable Near-Infrared Emission: Observation of Post-Synthesis Self-Narrowing of the Particle Size Distribution, Adv. Mater. 15 (21) (2003) 1844–1849.

[30] J. Park, J. Joo, S.G. Kwon, Y. Jang, T. Hyeon, Synthesis of Monodisperse Spherical Nanocrystals, Angew. Chemie Int. Ed. 46 (25) (2007) 4630–4660.

[31] S.G. Kwon, T. Hyeon, Colloidal Chemical Synthesis and Formation Kinetics of Uniformly Sized Nanocrystals of Metals, Oxides, and Chalcogenides, Acc. Chem. Res. 41 (12) (2008) 1696–1709.

[32] S.P. Shields, V.N. Richards, W.E. Buhro, Nucleation Control of Size and Dispersity in Aggregative Nanoparticle Growth. A Study of the Coarsening Kinetics of Thiolate-Capped Gold Nanocrystals, Chem. Mater. 22 (10) (2010) 3212–3225.

[33] D.B.K. Chu, J.S. Owen, B. Peters, Nucleation and Growth Kinetics from LaMer Burst Data, J. Phys. Chem. A 121 (40) (2017) 7511–7517.

[34] X. Wang, Y. Li, Monodisperse Nanocrystals: General Synthesis, Assembly, and Their Applications, Chem. Commun. No. 28 (2007) 2901.

[35] E.A. Slejko, L. Cozzarini, V. Lughi, Engineering of Colloidal Nanocrystal Thin Films and Their Optoelectronic Properties: A Simple and Effective Route, Nano-Structures & Nano-Objects 22 (2020), 100432.

[36] K. Miszta, J. De Graaf, G. Bertoni, D. Dorfs, R. Brescia, S. Marras, L. Ceseracciu, R. Cingolani, R. Van Roij, M. Dijkstra, L. Manna, Hierarchical Self-Assembly of Suspended Branched Colloidal Nanocrystals into Superlattice Structures, Nat. Mater. 10 (11) (2011) 872–876.

[37] K. Thorkelsson, P. Bai, T. Xu, Self-Assembly and Applications of Anisotropic Nanomaterials: A Review, Nano Today 10 (1) (2015) 48–66.

[38] E.A. Slejko, V. Lughi, Upconversion Photoluminescence in Colloidal CdSe/CdS Nanocrystal-Based Solid Films, Nano-Structures and Nano-Objects 26 (2021), 100742.

[39] T.J. Woehl, C. Park, J.E. Evans, I. Arslan, W.D. Ristenpart, N.D. Browning, Direct Observation of Aggregative Nanoparticle Growth: Kinetic Modeling of the Size Distribution and Growth Rate, Nano Lett. 14 (1) (2014) 373–378.

[40] H. Zheng, R.K. Smith, Y. Jun, C. Kisielowski, U. Dahmen, A.P. Alivisatos, Observation of Single Colloidal Platinum Nanocrystal Growth Trajectories, Science. 324 (5932) (2009) 1309–1312.

[41] N. Razgoniaeva, M. Yang, P. Garrett, N. Kholmicheva, P. Moroz, H. Eckard, L. Royo Romero, D. Porotnikov, D. Khon, M. Zamkov, Just Add Ligands: Self-Sustained Size Focusing of Colloidal Semiconductor Nanocrystals, Chem. Mater. 30 (4) (2018) 1391–1398.

[42] J. Polte, R. Erler, A.F. Thünemann, S. Sokolov, T.T. Ahner, K. Rademann, F. Emmerling, R. Kraehnert, Nucleation and Growth of Gold Nanoparticles Studied via in Situ Small Angle X-Ray Scattering at Millisecond Time Resolution, ACS Nano 4 (2) (2010) 1076–1082.

[43] J. Polte, X. Tuaev, M. Wuithschick, A. Fischer, A.F. Thuenemann, K. Rademann, R. Kraehnert, F. Emmerling, Formation Mechanism of Colloidal Silver Nanoparticles: Analogies and Differences to the Growth of Gold Nanoparticles, ACS Nano 6 (7) (2012) 5791–5802.

[44] S. Busatto, M. de Ruiter, J.T.B.H. Jastrzebski, W. Albrecht, V. Pinchetti, S. Brovelli, S. Bals, M.-E. Moret, C. de Mello Donega, Luminescent Colloidal InSb Quantum Dots from In Situ Generated Single-Source Precursor, ACS Nano 14 (10) (2020) 13146–13160.

[45] H.-G. Liao, L. Cui, S. Whitelam, H. Zheng, Real-Time Imaging of Pt 3 Fe Nanorod Growth in Solution, Science. 336 (6084) (2012) 1011–1014.

[46] J.M. Grogan, L. Rotkina, H.H. Bau, In Situ Liquid-Cell Electron Microscopy of Colloid Aggregation and Growth Dynamics, Phys. Rev. E 83 (6) (2011), 061405.

[47] L.R. Parent, D.B. Robinson, T.J. Woehl, W.D. Ristenpart, J.E. Evans, N. D. Browning, I. Arslan, Direct in Situ Observation of Nanoparticle Synthesis in a Liquid Crystal Surfactant Template, ACS Nano 6 (4) (2012) 3589–3596.

[48] D. Li, M.H. Nielsen, J.R.I. Lee, C. Frandsen, J.F. Banfield, J.J. De Yoreo, Direction-Specific Interactions Control Crystal Growth by Oriented Attachment, Science. 336 (6084) (2012) 1014–1018.

[49] E.A. Slejko, V. Lughi, Size Control at Maximum Yield and Growth Kinetics of Colloidal II–VI Semiconductor Nanocrystals, J. Phys. Chem. C 123 (2) (2019) 1421–1428.

[50] J.T. Siy, M.H. Bartl, Insights into Reversible Dissolution of Colloidal CdSe Nanocrystal Quantum Dots, Chem. Mater. 22 (21) (2010) 5973–5982.

[51] E.M. Brauser, T.D. Hull, J.D. McLennan, J.T. Siy, M.H. Bartl, Experimental Evaluation of Kinetic and Thermodynamic Reaction Parameters of Colloidal Nanocrystals, Chem. Mater. 28 (11) (2016) 3831–3838.

[52] J.S. Owen, E.M. Chan, H. Liu, A.P. Alivisatos, Precursor Conversion Kinetics and the Nucleation of Cadmium Selenide Nanocrystals, J. Am. Chem. Soc. 132 (51) (2010) 18206–18213.

[53] Z. Wan, H. Yang, W. Luan, S. Tu, tung, X. Zhou, Facile Synthesis of Monodisperse CdS Nanocrystals via Microreaction, Nanoscale Res. Lett. 5 (1) (2010) 130–137.

[54] N.G. Bastús, J. Comenge, V. Puntes, Kinetically Controlled Seeded Growth Synthesis of Citrate-Stabilized Gold Nanoparticles of up to 200 Nm: Size Focusing versus Ostwald Ripening, Langmuir 27 (17) (2011) 11098–11105.
[55] J. Piella, N.G. Bastús, V. Puntes, Size-Controlled Synthesis of Sub-10-Nanometer Citrate-Stabilized Gold Nanoparticles and Related Optical Properties, Chem. Mater. 28 (4) (2016) 1066–1075.
[56] N.G. Bastús, F. Merkoçi, J. Piella, V. Puntes, Synthesis of Highly Monodisperse Citrate-Stabilized Silver Nanoparticles of up to 200 Nm: Kinetic Control and Catalytic Properties, Chem. Mater. 26 (9) (2014) 2836–2846.
[57] J. Zhang, J. Gao, E.M. Miller, J.M. Luther, M.C. Beard, Diffusion-Controlled Synthesis of PbS and PbSe Quantum Dots with in Situ Halide Passivation for Quantum Dot Solar Cells, ACS Nano 8 (1) (2014) 614–622.
[58] G.G. Yordanov, C.D. Dushkin, E. Adachi, Early Time Ripening during the Growth of CdSe Nanocrystals in Liquid Paraffin, Colloids Surfaces A Physicochem. Eng. Asp. 316 (1–3) (2008) 37–45.
[59] Y. Zhang, C. Zhang, C. Xu, X. Wang, C. Liu, G.I.N. Waterhouse, Y. Wang, H. Yin, Ultrasmall Au Nanoclusters for Biomedical and Biosensing Applications: A Mini-Review, Talanta 200 (March) (2019) 432–442.
[60] J. Polte, Fundamental Growth Principles of Colloidal Metal Nanoparticles – a New Perspective, CrystEngComm 17 (36) (2015) 6809–6830.
[61] T. Wen, L.N. Brush, K.M. Krishnan, A Generalized Diffusion Model for Growth of Nanoparticles Synthesized by Colloidal Methods, J. Colloid Interface Sci. 419 (2014) 79–85.
[62] N.T.K. Thanh, N. Maclean, S. Mahiddine, Mechanisms of nucleation and growth of nanoparticles in solution, Chem. Rev. 114 (15) (2014) 7610–7630.
[63] S. Lazzari, M. Abolhasani, K.F. Jensen, Modeling of the Formation Kinetics and Size Distribution Evolution of II–VI Quantum Dots, React. Chem. Eng. 2 (4) (2017) 567–576.
[64] V.K. La Mer, Nucleation in Phase Transitions, Ind. Eng. Chem. 44 (6) (1952) 1270–1277.
[65] T. Sugimoto, Preparation of Monodispersed Colloidal Particles, Adv. Colloid Interface Sci. 28 (1987) 65–108.
[66] L. Zargarzadeh, J.A.W. Elliott, Thermodynamics of Surface Nanobubbles, Langmuir 32 (43) (2016) 11309–11320.
[67] S.I. Koshoridze, Y.K. Levin, Bubble Formation on a Hydrophobic Surface, Tech. Phys. 65 (6) (2020) 846–850.
[68] A.L. Rogach, Semiconductor Nanocrystal Quantum Dots; Rogach, A. L., Ed.; Springer Vienna: Vienna, 2008.
[69] J. van Embden, P. Mulvaney, Nucleation and Growth of CdSe Nanocrystals in a Binary Ligand System, Langmuir 21 (22) (2005) 10226–10233.
[70] P. Reiss, M. Carrière, C. Lincheneau, L. Vaure, S. Tamang, Synthesis of semiconductor nanocrystals, focusing on nontoxic and earth-abundant materials, Chem. Rev. 116 (18) (2016) 10731–10819.
[71] A. Shrestha, N.A. Spooner, S.Z. Qiao, S. Dai, Mechanistic insight into the nucleation and growth of oleic acid capped lead sulphide quantum dots, Phys. Chem. Chem. Phys. 18 (20) (2016) 14055–14062.
[72] G. Kaptay, The Chemical (Not Mechanical) Paradigm of Thermodynamics of Colloid and Interface Science, Adv. Colloid Interface Sci. 256 (2018) 163–192.
[73] R. García-Rodríguez, M.P. Hendricks, B.M. Cossairt, H. Liu, J.S. Owen, Conversion Reactions of Cadmium Chalcogenide Nanocrystal Precursors, Chem. Mater. 25 (8) (2013) 1233–1249.
[74] K. De Nolf, R.K. Čapek, S. Abe, M. Sluydts, Y. Jang, J.C. Martins, S. Cottenier, E. Lifshitz, Z. Hens, Controlling the Size of Hot Injection Made Nanocrystals by Manipulating the Diffusion Coefficient of the Solute, J. Am. Chem. Soc. 137 (7) (2015) 2495–2505.
[75] J.Y. Rempel, M.G. Bawendi, K.F. Jensen, Insights into the Kinetics of Semiconductor Nanocrystal Nucleation and Growth, J. Am. Chem. Soc. 131 (12) (2009) 4479–4489.
[76] X. Peng, J. Wickham, A.P. Alivisatos, Kinetics of II-VI and III-V Colloidal Semiconductor Nanocrystal Growth: "Focusing" of Size Distributions, J. Am. Chem. Soc. 120 (21) (1998) 5343–5344.